ACCOUNTS of chemical research

Article

Cite This: Acc. Chem. Res. 2018, 51, 3023−3030

pubs.acs.org/accounts

Harnessing Medium Anisotropy To Control Active Matter

Published as part of the Accounts of Chemical Research special issue "Fundamental Aspects of Self-Powered Nano- and Micromotors".

Igor S. Aranson*

Departments of Biomedical Engineering, Chemistry and Mathematics, Pennsylvania State University, University Park, Pennsylvania 16802, United States

CONSPECTUS: Active matter is a wide class of nonequilibrium systems consisting of interacting self-propelled agents transducing the energy stored in the environment into mechanical motion. Numerous examples range from microscopic cytoskeletal filaments and swimming organisms (bacteria and unicellular algae), synthetic catalytic nanomotors, colloidal self-propelled Janus particles, to macroscopic bird flocks, fish schools, and even human crowds. Active matter demonstrates a remarkable tendency toward self-organization and development of collective states with the long-range spatial order. Furthermore, active materials exhibit properties that are not present in traditional materials like plastics or ceramics: self-repair, shape change, and adaptation.

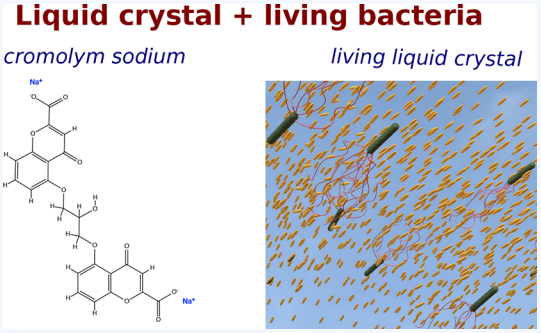

A suspension of microscopic swimmers, such as motile bacteria or self-propelled colloids (active suspensions), is possibly the simplest and the most explored realization of active matter. Recent studies of active suspensions revealed a wealth of unexpected behaviors, from a dramatic reduction of the effective viscosity, enhanced mixing and self-diffusion, rectification of chaotic motion, to artificial rheotaxis (drift against the imposed flow) and cross-stream migration. To date, most of the studies of active matter are performed in isotropic suspending medium, like water with the addition of some "fuel", e.g., nutrient for bacteria or H_2O_2 for catalytic bimetallic AuPt nanorods. A highly structured anisotropic suspending medium represented by lyotropic liquid crystal (water-soluble) opens enormous opportunities to control and manipulate active matter.

Liquid crystals exhibit properties intermediate between solid and liquids; they may flow like a liquid but respond to deformations as a solid due to a crystal-like orientation of molecules. Liquid crystals doped by a small amount of active component represent a new class of composite materials (living liquid crystals or LLCs) with unusual mechanical and optical properties. LLCs demonstrate a variety of highly organized dynamic collective states, spontaneous formation of dynamic textures of topological defects (singularities of local molecular orientation), controlled and reconfigurable transport of cargo particles, manipulation of individual trajectories of microswimmers, and many others. Besides insights into fundamental mechanisms governing active materials, living liquid crystals may have intriguing applications, such as the design of new classes of soft adaptive bioinspired materials capable to respond to physical and chemical stimuli, such as light, magnetic, and electric fields, mechanical shear, airborne pollutants, and bacterial toxins. This Account details the most recent developments in the field of LLCs and discusses how the anisotropy of liquid crystals can be harnessed to control and manipulate active materials.

1. INTRODUCTION

Active matter is rapidly growing interdisciplinary field dealing with a broad class of self-organizing systems out of equilibrium; for reviews from different perspectives, see refs 1−6. Research in active matter focuses on the individual and collective behavior of living and synthetic self-propelled agents, from suspensions of micro-organisms,[7,8] cytoskeletal biological filaments and protein motors,[9−11] synthetic self-phoretic colloids[12−14] to macroscopic bird flocks, fish schools, and even human crowds.[15−17]

Suspensions of self-propelled particles like swimming bacteria or synthetic swimmers are among the simplest and the most characterized realizations of active matter. Extensive experimental and theoretical studies revealed the onset of collective behavior and "bacterial turbulence",[7,8,18−21] reduction of the effective viscosity,[22,23] active clustering,[13] artificial rheotaxis[24,25] and many other phenomena not present in equilibrium colloidal suspensions. A common wisdom is that the above phenomena arise due to an interplay of main fundamental physical mechanisms: self-propulsion of individual agents, short-range steric collisions, and long-range hydrodynamic interactions.[2,18,19,26] Furthermore, random reorientations of the microswimmers, either due to thermal noise or intrinsic mechanisms such as random tumbling of a bacterium[27] or flipping of a synthetic nanorod,[28] also affect the onset of collective behavior.[19]

Received: June 22, 2018
Published: October 31, 2018

DOI: 10.1021/acs.accounts.8b00300
Acc. Chem. Res. 2018, 51, 3023−3030

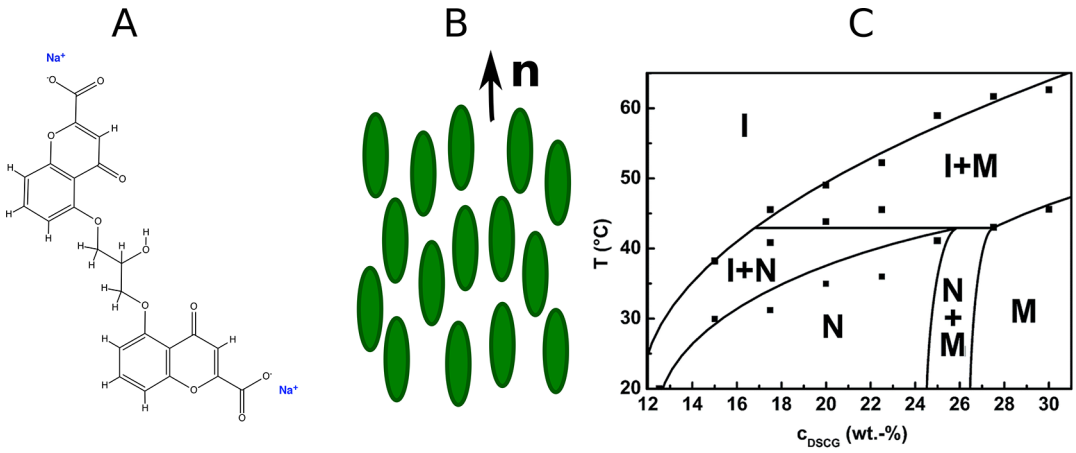

Figure 1. Lyotropic liquid crystal. (A) Two-dimensional (2D) structure of disodium cromoglycate (DSCG). (B) In water, the disclike DSCG molecules stack on a top of each other and form linear rodlike aggregates. In the nematic phase, the molecules have average orientation order characterize by the unit vector **n** (director). (C) Depending on temperature and amount of mesogenic material c_{DSCG}, the aggregates form various liquid crystalline phases: nematic (N), isotropic (I), and columnar (M). Panel (C) reproduced with permission from ref 63. Copyright 2015 Royal Society of Chemistry.

The so-called "active nematic" is another important and distinct class of lifelike material exemplified by nonmotile but otherwise active particles with apolar (or nematic) interactions. The most known example of an active nematic is a suspension of kinesin molecular motors and microtubules in the presence of "fuel" (adenosine triphosphate, ATP) and a crowding agent polyethylene glycol (PEG).[29] Another realization of an active nematic is a sheet of short actin filaments driven by clusters of myosin II motors.[30] While individual particles (microtubules) are polar (they have distinct "+" and "−" ends), in the absence of kinesin molecular motors they remain nonmotile and only exhibit Brownian diffusion. However, attachment of active kinesin clusters to a pair of microtubules of opposite polarity leads to the relative sliding and the overall displacement of the centers of mass of individual microtubules. The relative sliding induces so-called "active stresses" on the surrounding medium and drives self-organization. The presence of PEG promotes the formation of microtubule bundles and the onset of liquid crystalline (or nematic) order;[29] see also for recent reviews refs 31 and 32.

Active nematics exhibit complex spatiotemporal behavior,[33] long-range ordering of topological defects,[34] and nontrivial coupling between topology and activity.[35] A qualitative understanding of active nematics was achieved by particle simulations[36] and phenomenological models based on hydrodynamic approaches.[37,38] Near the onset of nematic order, asymptotic reduction of the probabilistic Boltzmann equation for interacting particles leads to the coarse-grained Ginzburg–Landau-type model.[39,40] Furthermore, a theoretical description based on the equilibrium model for liquid crystals[41−43] supplemented by a phenomenological "active stress" due to mutual sliding of microtubules was used in refs 44−48. These studies provided some important insights into the annihilation dynamics of defects, velocity correlations, and the onset of "active turbulence". However, it is not clear to what extent the equilibrium model for liquid crystals can be used for such an out-of-equilibrium system, how the continuum models are connected to the experiment,[29] and how model parameters are related to the experimental conditions.

Living liquid crystal (LLC) is a biosynthetic active composite represented by a suspension of microswimmers like bacteria in a nontoxic lyotropic liquid crystal.[49−53] The material combines highly structured synthetic liquid crystal and a small amount of "active dopant" (i.e., bacteria). The studies revealed unique optical and mechanical properties of LLCs, such as (i) guidance of bacteria along the nematic director, (ii) visualization of nanometer-thick bacterial flagella,[49] (iii) transport of cargo along bacterial trajectories,[50,54] (iv) dynamic self-assembly of bacterial clusters,[52] and (v) spinning to swimming transitions.[55] For higher bacterial concentrations, a variety of collective effects were observed: (i) the spontaneous onset of spatiotemporal director undulations, the proliferation of topological defects, and turbulent-like states,[49] (ii) trapping and transport of bacteria in the cores of topological defects,[56] and (iii) separation of topological defects at the isotropic–nematic interfaces.[57] There are other active systems sharing similarities with LLCs. The examples include motility assays (microtubules or actin filaments propelled by a carper of molecular motors),[10,11] living tissues of motile cells,[58,59] and colonies of gliding myxobacteria.[60,61]

Despite the similarities between dynamic states in LLCs and a sliding microtubules system in ref 29, the physical mechanisms governing the self-organization in these two active systems are very different. In contrast with the sliding microtubule system,[29] microswimmers like bacteria are self-propelled objects. As a result, the energy injection at a microscopic scale is provided by the rotation of bacterial flagella rather than the sliding of nearby microtubules. Furthermore, there is no direct mechanical coupling between orientation of bacteria and liquid crystal molecules: swimming bacteria interact with the liquid crystal by hydrodynamic and elastic forces. Therefore, the utility of generic phenomenological models of an active nematic[44−48] to LLCs is somewhat limited. More elaborate and specialized theoretical approaches incorporating the well-established model for nematic liquid crystal[43] coupled to the concentration evolution of self-propelled particles were established in refs 56 and 57.

2. LYOTROPIC LIQUID CRYSTALS

LLCs are formed by combining nontoxic lyotropic liquid crystal DSCG (disodium cromoglycate, $C_{23}H_{14}Na_2O_{11}$), see Figure 1A, with motile nonvirulent flagellated bacteria *Bacillus*

DOI: 10.1021/acs.accounts.8b00300
Acc. Chem. Res. 2018, 51, 3023−3030

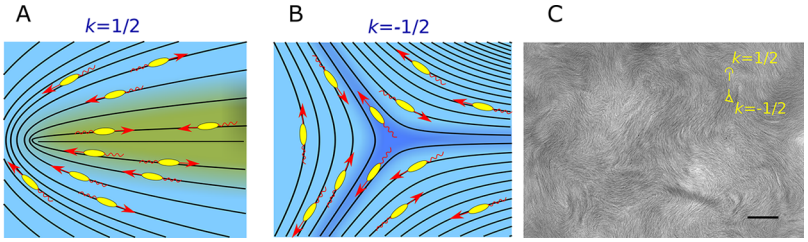

Figure 2. Half-integer topological defects. (A) Pointed (k = 1/2) defect. (B) Triangular (k = −1/2) defect. Panels (A) and (B) are reproduced from ref 56. Copyright 2017 American Physical Society. (C) Dynamic texture of topological defects formed in free-standing LLC film. Two nearby defects are highlighted. Bacteria are aligned along the local nematic director, as shown by the fine stripes. Scale bar: 30 μm. Panel (C) reproduced with permission from ref 49. Copyright 2014 National Academy of Sciences.

subtilis. DSCG is commonly used as an antiasthmatic drug. A lyotropic liquid crystal is formed by dissolving an amphiphilic mesogen in a suitable solvent. Under appropriate concentration, temperature and pressure conditions, various liquid crystalline phases are formed due to self-assembly of polar disc-like molecules of DSCG into linear nanometer-sized aggregates (so-called chromonics),[62,63] Figure 1B, C. In the simplest liquid crystalline phase, a nematic, the molecules have average orientational order characterized by the unit vector **n** (director), but no positional ordering. Since the head and tail of a molecule are indistinguishable, directions **n** and −**n** are equivalent. Other lyotropic liquid crystals were explored, e.g., Sunset Yellow FCF ($C_{16}H_{10}N_2Na_2O_7S_2$, a food additive). However, it appears to be toxic to bacteria.

3. TOPOLOGICAL DEFECTS

Topologically stable defects are typically associated with certain nonuniform configurations of the director **n** that cannot be removed by a continuous transformation.[42] Simply speaking, one may need to melt the entire liquid crystal in order to destroy the defect.

Dynamic textures of point topological defects appear spontaneously in LLCs if the concentration of bacteria, i.e., the activity, exceeds a certain threshold.[49] In this context, topological defects are point singularities of the director field **n**.[42] In two dimensions, topological defects are characterized by a topological charge k:

$$k = \frac{1}{2\pi}\oint_\Gamma \nabla\theta \cdot d\mathbf{l} = \frac{1}{2\pi}\oint_\Gamma d\theta \tag{1}$$

where θ is the orientation angle, $\mathbf{n} = (\cos(\theta),\sin(\theta))$, Γ is an arbitrary contour encircling the point of singularity, and **l** is the length element along the contour Γ. Topological charge measures how many multiples of 2π the director field rotates after encircling the singularity point. Correspondingly, due to the continuity condition, vector fields (e.g., magnetization) allow only integer values of the topological charge k. The equivalence of $\mathbf{n} \leftrightarrow -\mathbf{n}$ implies that half-integer topological defects with $k = \pm 1/2$, or disclinations, are also possible in nematics; see Figure 2.

In equilibrium homogeneous liquid crystals, isolated topological defects are at rest. If the equilibrium is perturbed, migration of topological defects decreases the free energy and brings the system back to equilibrium. The situation is more subtle in intrinsically nonequilibrium systems such as LLCs or active nematic. One may argue on the grounds of symmetry that if the system is homogeneous, negative (i.e triangular) defects should remain at rest because of the symmetric distribution of active component, i.e., bacteria in this case. In contrast, positive (or pointed) defects should move spontaneously due to nonsymmetric activity distribution.[33,44,64,65] Thus, 1/2 defects become self-propelled entities moving typically in the direction of the pointed end. Due to the interaction between the defects, negative defects may become entrained as well. However, the typical speed of negative defects remains significantly smaller than that of the positive ones.

4. CARGO TRANSPORT

Individual bacteria tend to be swimming along the LC director **n**.[49,51,52] If a bacterium becomes misaligned, it rapidly readjusts its body orientation in order to minimize the director distribution and corresponding elastic energy penalty. The relaxation time τ_0 can be estimated from the balance of viscous and elastic torques. According to ref 56, the relaxation time is

$$\tau_0 \approx \frac{\bar{\eta} l^2}{12K} \frac{\ln(2l/r)}{\ln(l/2r) - 1/2} \tag{2}$$

For typical experimental values for lyotropic chromonic liquid crystals such as DSCG,[66] viscosity is $\bar{\eta}$ = 4−5 kg m^{-1} s^{-1}, average elastic constant is K = 15 pN, and length and diameter of the bacterial body are l = 5 μm, r = 0.4 μm. It yields an estimate $\tau_0 \approx$ 1−1.5 s. Since the relaxation time τ_0 (of the order of a second) is small compared to the overall transport time, bacteria rapidly align with the director **n**. This rapid alignment enables cargo transport by bacteria; see Figure 3. Since the bacteria travel along the director, they push the desired cargo particles (2−3 μm polystyrene bead; see Figure

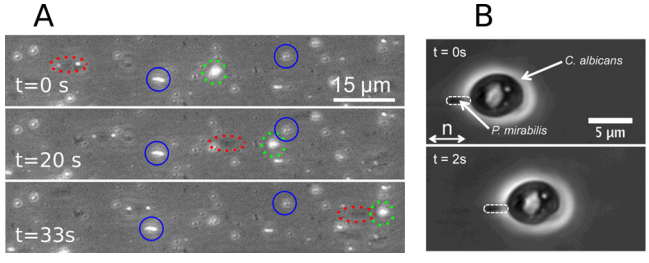

Figure 3. Cargo transport. (A) A single *Bacillus subtilis* bacterium (marked by a red dashed ellipse) pushes a fluorescent tracer (green dashed circle) along the bacterial path. Particles located slightly off the bacterial path (blue circles) are not affected. Panel (A) reproduced with permission from ref 50. Copyright 2015 American Physical Society. (B) A single *Proteus mirabilis* bacterium pushes a single fungal cell *Candida albicans* along the nematic director **n**. Panel (B) reproduced with permission from ref 54. Copyright 2015 Royal Society of Chemistry.

DOI: 10.1021/acs.accounts.8b00300
Acc. Chem. Res. 2018, 51, 3023−3030

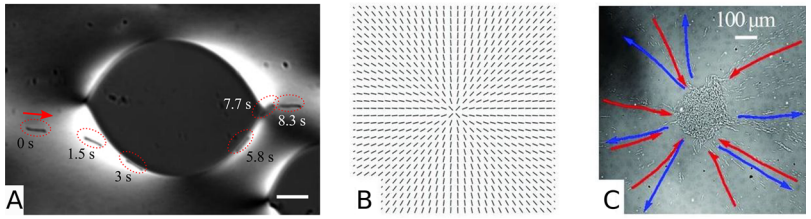

Figure 4. Manipulation of trajectories. (A) Trajectory of a single bacterium *Bacillus subtilis* around a tactoid, Scale bar 10 μm. Panel (A) reproduced with permission from ref 49. Copyright 2014 National Academy of Sciences. (B, C) Controlling bacterial transport by imprinted director pattern. (B) Imposed pure splay director distribution. (C) Radial trajectories of bacteria moving toward and away from the center and accumulating in the center. Panels (B and (C) reproduced from ref 69. Copyright 2016 AAAS.

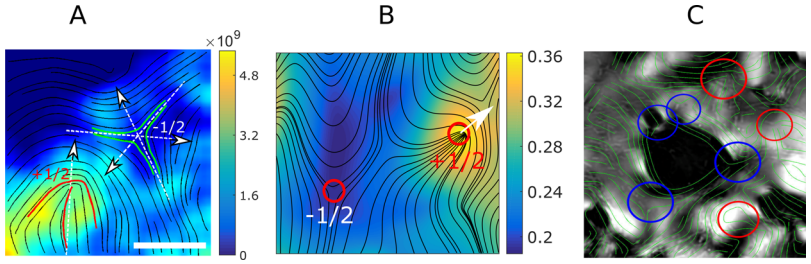

Figure 5. Concentration distributions. (A) Experiment: bacterial concentration distribution in the area containing two defects. Colors represent the concentration of bacteria extracted from the averaged fluorescence intensity. Two topological defects (1/2 and −1/2) are highlighted. White lines show defect orientations. Scale bar: 50 μm. (B) Computational model: Close-up view of the concentration field. Some defects are shown in red circles, and white arrow indicates the direction of motion. Panels (A) and (B) are reproduced from ref 56. Copyright 2017 American Physical Society. (C) Experimental nematic configuration around a single tactoid. Positive defects are indicated with red circles, negative with blue circles. Negative defects decorate the isotropic−nematic interface, whereas positive defects occur predominately in the bulk of the nematic phase. Panel (C) reproduced with permission from ref 57. Copyright 2018 Institute of Physics.

3A) or even large fungal cells (5 μm round cell; Figure 3B) as long as they are located along the bacterial path. Particles that are even slightly off the path are not affected.[50] Thus, bacteria can deliver a cargo exceeding the size of the bacterial body (4−5 μm). In contrast, significantly bigger algae-powered microswimmers can deliver a cargo of the size of 1 μm.[67] Cargo-delivering capability of bacteria is probably comparable to that of Janus nanomotors,[68] however bacteria exhibit more directed motion.

5. MANIPULATING TRAJECTORIES

Anisotropy of LLCs opens an opportunity to manipulate trajectories of individual bacteria by creating a desired director pattern. As it was established in refs 49 and 52, the bacteria can be guided along isotropic−nematic interfaces. As the temperature increases, LLCs approach a biphasic region, in which the isotropic and nematic phases coexist, Figure 1C. The isotropic regions appear as elongated dark droplets or "'negative tactoids"' (Figure 4A) aligned along the overall nematic director.[42,62] The isotropic tactoids distort the director around them and change the trajectories of bacteria: far from the tactoid, a bacterium swims along a straight line. When approaching the tactoid, the bacterium deviates from the straight line and follows the local distorted director. After a collision with the tactoid, the bacterium closely follows the curved tactoid's boundary and finally escapes at the cusp. The guidance of microswimmers by the nematic−isotropic interfaces and the overall director distribution in LLC offers intriguing design concepts of reconfigurable microfluidic devices. The bacterial trajectories can be engineered by local dynamic heating (for example, with focused laser beams).

Desired spatially varying patterns of liquid crystal orientation can be created through controlled surface alignment of the director.[69] The methodology developed in refs 69 and 70 allows the designing of director patterns with well-defined deformations, either pure bend, pure splay, or mixed splay−bend. To imprint the patterns, the bounding plates are pretreated to impose the desired surface alignment of the adjacent liquid crystal.[70] Shortly, the procedure includes coating the plates with a layer of photosensitive molecules, and irradiation of the layer with a linearly polarized light beam that changes from point to point. The irradiation forces the photosensitive molecules to align in accordance with local polarization. Consequently, the photoaligned surface molecules force alignment of the director in the bulk. This imposed director pattern guides bacteria in the desired direction, Figure 4B, C.

A similar strategy is also applied to manipulate the trajectory of colloidal particles in nematic liquid crystals.[71] The colloids can be driven by electrophoretic mechanism via application of the alternating electric field.[72] Arbitrary reconfigurable paths can be imprinted by irradiation with UV or blue light. Depending on the imprinted pattern topology, motile colloids can be organized in radial asters, rotating vortices, and other dynamic structures.[71]

6. CONTROLLING TOPOLOGICAL DEFECTS

Topological defects, or singularities of the molecular orientation field **n**,[42] strongly influence the spatiotemporal behavior of active media. Since the topological defects cannot appear or disappear spontaneously (opposite defects are created and annihilated in pairs), they can be viewed as fundamental nonlinear excitations that orchestrate the overall dynamics of the medium. In equilibrium (or passive) systems, topological defects appear as a result of a phase transition. Similarly, pairs of topological defects appear spontaneously if

DOI: 10.1021/acs.accounts.8b00300
Acc. Chem. Res. 2018, 51, 3023−3030

the activity (e.g., concentration of bacteria) exceeds a certain threshold.

In contrast to passive systems, +1/2 active defects are self-propelled due to a nonsymmetric distribution of activity whereas isolated −1/2 defects are immobile; see Figure 2. Similarly to oppositely charged particles, negative and positive defects attract each other end eventually annihilate. However, the activity of the system leads to the nucleation of new defect pairs. Recombining/unbinding pairs of ±1/2 defects can be observed in a wide range of bacterial concentrations.

At the onset of active turbulence, +1/2 defects attain a fraction of the average speed of bacteria, i.e., about 2−3 μm/s. The speed of −1/2 defects near the onset remains about 1/5 of the speed of positive defects. With the increase in bacterial concentration, the speed of both negative and positive defects monotonously increases and becomes comparable with the speed of bacteria, i.e., 20−30 μm/s.

Experimental and theoretical studies of LLC in ref 56 revealed a surprising relation between activity and topology: 1/2 defects trap bacteria in their cores while −1/2 defects expel bacteria, Figure 5. The effect depends on the overall activity of LLC and is the most pronounced near the threshold of instability when the defect speed is minimal. It fades away with the increase in bacterial concentration.

The phenomenon of accumulation and depletion is directly related to director topology at the defect cores. Since the nematic orientation contour lines, and, respectively, the bacterial trajectories, converge at the core of the +1/2 defect, bacteria swimming toward the defect accumulate in the core, Figure 2A. Correspondingly, bacteria swimming in the opposite direction will leave the defect, leading to an overall increase in the concentration. In contrast, the nematic configuration of −1/2 defect expels the bacteria independently of their orientation (Figure 2B): bacteria close to the defect core (in dark blue region) swim away and bacteria swimming toward the defect are deflected.

Accumulation of the bacteria in the core of 1/2 defects can be used to capture and transport active particles in the overall turbulent state. Since the defects typically move perpendicular to the averaged nematic direction,[42] defects can be guided by the imposed nematic pattern. Furthermore, the motion of defects is affected by the isotropic−nematic (I−N) interfaces.[57] Namely, the I−N interfaces predominately trap negative defects whereas positive defects stay in the bulk of the nematic phase. This phenomenon is explained by the different mobility of positive and negative defects: positive defects are self-propelled and can easily overcome a potential barrier at the I−N interface. Negative defects are stationary and are easily trapped at the interfaces. As a consequence, this effect leads to accumulation of negative defects near normal tactoids, Figure 5C. Thus, by designing a pattern of normal inclusions one can suppress the motion of negative defects and enhance the transport of positive defects.

7. MOTION IN 3D

The liquid crystalline environment also allows the control of swimmer trajectories in 3D by forcing the bacteria to swim along the director. Nematic orientation in the bulk can be effectively tuned by the surface alignment (anchoring). If the anchoring favors planar alignment (i.e., parallel to the surface), then the bacteria are essentially confined in the middle of a sandwich-like cell due to elastic repulsion from the bounding plates.[73]

If the alignment is homeotropic (i.e., perpendicular to the wall), the LC director forces the bacteria to travel in the bulk, perpendicular to the walls. LLCs with homeotropic anchoring were studied in ref 55. To ensure perpendicular alignment of the molecules at the substrate, the glass surfaces of the sandwich-like cell were treated with a water solution containing 0.4 wt % *N*,*N*-dimethyl-*N*-octadecyl-3-aminopropyl trimethoxysilyl chloride $[(CH_3O)_3Si(CH_2)_3N\text{-}(CH_3)_2(CH_2)_{17}CH_3]Cl$ and 0.1 wt % H_2SO_4.[74] Alternatively, homeotropic alignment was achieved by the growth of graphene monolayers on Cu foils via chemical vapor deposition and the consequent transfer of them onto the glass substrate.[53]

The studies of LLCs in thin sandwich-like cells with homeotropic anchoring demonstrated that the bacteria can overcome the stabilizing elastic forces and swim perpendicularly to the imposed director, i.e., parallel to the bounding plates. This effect can be explained by a finite surface director anchoring strength at the bacterial body.[55] It leads to the coexistence of vertical spinning states, or VSP (bacteria trapped due to perpendicular director orientation) and horizontal swimming state (HSW), Figure 6. The HSW

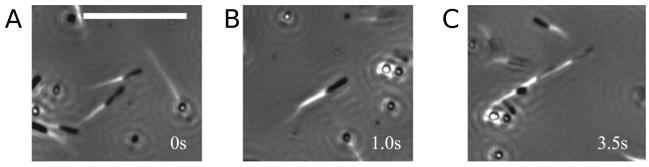

Figure 6. Coexistence of vertical spinning and horizontal swimming states in a homeotropic cell. Spinning bacteria are seen as dark dots, swimming bacteria seen as dark rods with a bright tail. Panels (A)−(C) illustrate end-to-end collective motion: two bacteria collide under a small angle, swim as a group, and then separate due to the difference in velocity. Scale bar: 20 μm. Panels (A)−(C) reproduced with permission from ref 55. Copyright 2017 Institute of Physics.

bacteria leave a bright trail due to the transient planar alignment of the director. This phenomenon facilitates the formation of temporary trainlike groups with end-to-end coordination. The bacteria tend to swim along the same trajectory, similar to ants following the same trail, Figure 6. In this case, leading bacterium creates director distortions that provide the guiding path to the following bacteria. Nontrivial 3D director distributions can be created in a hybrid cell, where one of the plates has homeotropic alignment, and another planar one.[53] In this cell, the bacteria are forced to swim near the cell with planar alignment.

It is an open question whether a similar strategy can be used for the 3D control of synthetic swimmers in liquid crystals. It is well-known that colloidal particles can be guided in the liquid crystalline environment by the applied electric or magnetic fields.[73] As the synthetic swimmers are concerned, most likely the liquid crystalline environment is not compatible with chemical propulsion mechanism of AuPt nanomotors. However, an interesting situation may arise in the case of thermophoretic Janus particles powered by light.[75] Birefringence and nontrivial optical properties of liquid crystals may result in complex swimming trajectory of light-propelled Janus particles.

DOI: 10.1021/acs.accounts.8b00300
Acc. Chem. Res. 2018, 51, 3023−3030

8. SUMMARY AND OUTLOOK

Here we surveyed various strategies for how the anisotropy of a liquid crystalline environment can be harnessed to control active motion. Besides insights into fundamental mechanisms governing active materials, living liquid crystals may have intriguing applications. They can potentially enable the design of new classes of soft adaptive bioinspired materials responding to physical and chemical stimuli, such as light, mechanical shear, airborne pollutants, and bacterial toxins. The recent developments also demonstrated that collective emergent properties of LLCs may yield a new class of active soft materials in which organization can be controlled via dissipation of energy.[76]

From a technological perspective, it is highly desirable to engineer a mimetic analog of LLCs, e.g., based on synthetic swimmers like catalytic AuPt nanorods[12] or other type of phoretic Janus particles, e.g. platinum-silica spheres.[75] It appears that the chemical composition of lyotropic LCs is generally not compatible with the propulsion mechanisms of AuPt nanorods. However, the liquid crystalline anisotropy can be used to control the motion of Janus particles, e.g., silica-palladium spheres, confined at the interface between nematic liquid crystals and the aqueous solution of H_2O_2.[77] In this respect, acoustic propulsion of nanorods by ultrasound[78,79] is easier to achieve. However, inhomogeneous spatial distribution of the ultrasound intensity makes the control of nanorod motion challenging. Furthermore, propulsion of colloidal particles in liquid crystals in can be also achieved by electric or magnetic fields; see for review ref 73. It is tempting to use liquid crystal anisotropy to guide, e.g., artificial magnetically propelled microswimmers.[80] However, this system was not realized yet, likely due to a high viscosity of liquid crystals. Thus, utilization of the liquid crystal anisotropy for 2D and 3D motion control of synthetic swimmers remains open challenge.

Another intriguing opportunity is to use more ordered LC phases, e.g., smectic (layered) or cholesteric (chiral) to control active motion. Preliminary experiments show that bacteria do not exhibit mobility in smectic or cholesteric LCs, likely due to increased viscosity. In addition to point topological defects in nematics, smectic LCs exhibit textures of more complex defects, such as focal conical domains (FCDs), i.e., surfaces whose lines of curvature are circles.[81] FCDs present new templates for the organization of active matter that can be controlled by surface patterning[82,83] or a magnetic field.[84]

One may expect many similarities between living and synthetic active matter systems. For example, bacteria and chemically powered nanomotors are similar in size, shape, and propulsion speeds. However, this similarity is somewhat superficial. There are many differences, especially in the interparticle interactions and especially in interactions with the boundaries. Bacteria often scatter from the boundaries or other cells.[85] In contrast, chemically propelled nanorods hover above negatively charged surfaces due to the electric dipole induced by electrochemical reactions.[25] As a result, living and synthetic active matters do not necessarily exhibit similar collective states and responses to external stimuli. For example, at sufficiently high concentrations, bacteria self-organize into large-scale vortices and jets[8] whereas chemically propelled rods from permanent clusters.[12,86]

Finally, common biological fluids, such as mucus,[87] DNA solutions,[88] and suspensions of viruses,[89] often exhibit a liquid crystalline order. For example, cervical mucus plays crucial roles in higher organisms, from aiding fertilization to protecting the female reproductive tract. Since mucus anisotropy and heterogeneity depend on how mechanical stress is applied, it affects the motility of bacteria in a nontrivial way.[90] Thus, understanding the interaction between bacteria and mucus is also important for human health.

AUTHOR INFORMATION

Corresponding Author

*E-mail: isa12@psu.edu.

ORCID

Igor S. Aranson: 0000-0002-4062-5393

Funding

The work was supported by the National Science Foundation DMS-1735700.

Notes

The author declares no competing financial interest.

Biography

Igor S. Aranson received his Ph.D. from Nizhniy Novgorod State University, former Soviet Union, and did postdoctoral work at the Institute for Applied Physics, Nizhniy Novgorod. He is the Huck Chair Professor of Biomedical Engineering, Chemistry and Mathematics at Penn State University. His research interests include active materials, computational modeling of cell motility, and applied mathematics.

ACKNOWLEDGMENTS

The author thanks Prof. Oleg D Lavrentovich for illuminating discussions.

REFERENCES

(1) Ramaswamy, S. The Mechanics and Statistics of Active Matter. *Annu. Rev. Condens. Matter Phys.* **2010**, *1*, 323−345.
(2) Aranson, I. S. Active colloids. *Phys.-Usp.* **2013**, *56*, 79.
(3) Lavrentovich, O. D. Active colloids in liquid crystals. *Curr. Opin. Colloid Interface Sci.* **2016**, *21*, 97−109.
(4) Zhang, J.; Luijten, E.; Grzybowski, B. A.; Granick, S. Active colloids with collective mobility status and research opportunities. *Chem. Soc. Rev.* **2017**, *46*, 5551−5569.
(5) Dey, K. K. Dynamic coupling at low Reynolds number. *Angew. Chem., Int. Ed.* **2018**, DOI: 10.1002/anie.201804599.
(6) Dey, K. K.; Sen, A. Chemically propelled molecules and machines. *J. Am. Chem. Soc.* **2017**, *139*, 7666−7676.
(7) Dombrowski, C.; Cisneros, L.; Chatkaew, S.; Goldstein, R. E.; Kessler, J. O. Self-concentration and large-scale coherence in bacterial dynamics. *Phys. Rev. Lett.* **2004**, *93*, 098103.
(8) Sokolov, A.; Aranson, I. S.; Kessler, J. O.; Goldstein, R. E. Concentration dependence of the collective dynamics of swimming bacteria. *Phys. Rev. Lett.* **2007**, *98*, 158102.
(9) Surrey, T.; Nédélec, F.; Leibler, S.; Karsenti, E. Physical properties determining self-organization of motors and microtubules. *Science* **2001**, *292*, 1167−1171.
(10) Schaller, V.; Weber, C.; Semmrich, C.; Frey, E.; Bausch, A. R. Polar patterns of driven filaments. *Nature* **2010**, *467*, 73−77.
(11) Sumino, Y.; Nagai, K. H.; Shitaka, Y.; Tanaka, D.; Yoshikawa, K.; Chaté, H.; Oiwa, K. Large-scale vortex lattice emerging from collectively moving microtubules. *Nature* **2012**, *483*, 448−452.
(12) Paxton, W. F.; Kistler, K. C.; Olmeda, C. C.; Sen, A.; St. Angelo, S. K.; Cao, Y.; Mallouk, T. E.; Lammert, P. E.; Crespi, V. H. Catalytic nanomotors: autonomous movement of striped nanorods. *J. Am. Chem. Soc.* **2004**, *126*, 13424−13431.

DOI: 10.1021/acs.accounts.8b00300
Acc. Chem. Res. 2018, 51, 3023−3030

(13) Palacci, J.; Sacanna, S.; Steinberg, A. P.; Pine, D. J.; Chaikin, P. M. Living crystals of light-activated colloidal surfers. *Science* **2013**, *339*, 936−940.
(14) Theurkauff, I.; Cottin-Bizonne, C.; Palacci, J.; Ybert, C.; Bocquet, L. Dynamic clustering in active colloidal suspensions with chemical signaling. *Phys. Rev. Lett.* **2012**, *108*, 268303.
(15) Cavagna, A.; Cimarelli, A.; Giardina, I.; Parisi, G.; Santagati, R.; Stefanini, F.; Viale, M. Scale-free correlations in starling flocks. *Proc. Natl. Acad. Sci. U. S. A.* **2010**, *107*, 11865−11870.
(16) Couzin, I. D.; Krause, J.; James, R.; Ruxton, G. D.; Franks, N. R. Collective memory and spatial sorting in animal groups. *J. Theor. Biol.* **2002**, *218*, 1−11.
(17) Karamouzas, I.; Skinner, B.; Guy, S. J. Universal power law governing pedestrian interactions. *Phys. Rev. Lett.* **2014**, *113*, 238701.
(18) Wensink, H. H.; Dunkel, J.; Heidenreich, S.; Drescher, K.; Goldstein, R. E.; Löwen, H.; Yeomans, J. M. Meso-scale turbulence in living fluids. *Proc. Natl. Acad. Sci. U. S. A.* **2012**, *109*, 14308−14313.
(19) Sokolov, A.; Aranson, I. S. Physical properties of collective motion in suspensions of bacteria. *Phys. Rev. Lett.* **2012**, *109*, 248109.
(20) Saintillan, D.; Shelley, M. J. Instabilities and pattern formation in active particle suspensions: kinetic theory and continuum simulations. *Phys. Rev. Lett.* **2008**, *100*, 178103.
(21) Aranson, I. S.; Sokolov, A.; Kessler, J. O.; Goldstein, R. E. Model for dynamical coherence in thin films of self-propelled microorganisms. *Phys. Rev. E* **2007**, *75*, 040901.
(22) Sokolov, A.; Aranson, I. S. Reduction of viscosity in suspension of swimming bacteria. *Phys. Rev. Lett.* **2009**, *103*, 148101.
(23) López, H. M.; Gachelin, J.; Douarche, C.; Auradou, H.; Clément, E. Turning bacteria suspensions into superfluids. *Phys. Rev. Lett.* **2015**, *115*, 028301.
(24) Palacci, J.; Sacanna, S.; Abramian, A.; Barral, J.; Hanson, K.; Grosberg, A. Y.; Pine, D. J.; Chaikin, P. M. Artificial rheotaxis. *Science advances* **2015**, *1*, e1400214.
(25) Ren, L.; Zhou, D.; Mao, Z.; Xu, P.; Huang, T. J.; Mallouk, T. E. Rheotaxis of Bimetallic Micromotors Driven by Chemical−Acoustic Hybrid Power. *ACS Nano* **2017**, *11*, 10591−10598.
(26) Bechinger, C.; Di Leonardo, R.; Löwen, H.; Reichhardt, C.; Volpe, G.; Volpe, G. Active particles in complex and crowded environments. *Rev. Mod. Phys.* **2016**, *88*, 045006.
(27) Berg, H. C.; Brown, D. A. Chemotaxis in Escherichia coli analysed by three-dimensional tracking. *Nature* **1972**, *239*, 500−504.
(28) Takagi, D.; Braunschweig, A. B.; Zhang, J.; Shelley, M. J. Dispersion of self-propelled rods undergoing fluctuation-driven flips. *Phys. Rev. Lett.* **2013**, *110*, 038301.
(29) Sanchez, T.; Chen, D. T.; DeCamp, S. J.; Heymann, M.; Dogic, Z. Spontaneous motion in hierarchically assembled active matter. *Nature* **2012**, *491*, 431−434.
(30) Kumar, N.; Zhang, R.; de Pablo, J. J.; Gardel, M. L. Tunable structure and dynamics of active liquid crystals. *Science Advances* **2018**, *4*, eaat7779.
(31) Needleman, D.; Dogic, Z. Active matter at the interface between materials science and cell biology. *Nature Reviews Materials* **2017**, *2*, 17048.
(32) Doostmohammadi, A.; Ignés-Mullol, J.; Yeomans, J. M.; Sagués, F. Active nematics. *Nat. Commun.* **2018**, *9*, 3246.
(33) Keber, F. C.; Loiseau, E.; Sanchez, T.; DeCamp, S.; Giomi, L.; Bowick, M. J.; Marchetti, M. C.; Dogic, Z.; Bausch, A. R. Topology and dynamics of active nematic vesicles. *Science* **2014**, *345*, 1135−1139.
(34) DeCamp, S. J.; Redner, G. S.; Baskaran, A.; Hagan, M. F.; Dogic, Z. Orientational order of motile defects in active nematics. *Nat. Mater.* **2015**, *14*, 1110−1115.
(35) Ellis, P. W.; Pearce, D. J.; Chang, Y.-W.; Goldsztein, G.; Giomi, L.; Fernandez-Nieves, A. Curvature-induced defect unbinding and dynamics in active nematic toroids. *Nat. Phys.* **2018**, *14*, 85.
(36) Gao, T.; Blackwell, R.; Glaser, M. A.; Betterton, M.; Shelley, M. J. Multiscale modeling and simulation of microtubule−motor-protein assemblies. *Phys. Rev. E* **2015**, *92*, 062709.
(37) Ramaswamy, S.; Simha, R. A.; Toner, J. Active nematics on a substrate: Giant number fluctuations and long-time tails. *Europhys. Lett.* **2003**, *62*, 196.
(38) Baskaran, A.; Marchetti, M. C. Hydrodynamics of self-propelled hard rods. *Phys. Rev. E* **2008**, *77*, 011920.
(39) Bertin, E.; Chaté, H.; Ginelli, F.; Mishra, S.; Peshkov, A.; Ramaswamy, S. Mesoscopic theory for fluctuating active nematics. *New J. Phys.* **2013**, *15*, 085032.
(40) Ngo, S.; Peshkov, A.; Aranson, I. S.; Bertin, E.; Ginelli, F.; Chaté, H. Large-scale chaos and fluctuations in active nematics. *Phys. Rev. Lett.* **2014**, *113*, 038302.
(41) de Gennes, P.-G.; Prost, J. *The physics of liquid crystals*; Oxford University Press, 1995; Vol. *83*.
(42) Kléman, M.; Lavrentovich, O. D. *Soft matter physics: an introduction*; Springer Science & Business Media, 2007.
(43) Beris, A. N.; Edwards, B. J. *Thermodynamics of flowing systems: With internal microstructure*; Oxford University Press on Demand, 1994.
(44) Giomi, L.; Bowick, M. J.; Ma, X.; Marchetti, M. C. Defect Annihilation and Proliferation in Active Nematics. *Phys. Rev. Lett.* **2013**, *110*, 228101.
(45) Thampi, S. P.; Golestanian, R.; Yeomans, J. M. Velocity Correlations in an Active Nematic. *Phys. Rev. Lett.* **2013**, *111*, 118101.
(46) Thampi, S. P.; Golestanian, R.; Yeomans, J. M. Active nematic materials with substrate friction. *Phys. Rev. E* **2014**, *90*, 062307.
(47) Blow, M. L.; Thampi, S. P.; Yeomans, J. M. Biphasic, Lyotropic, Active Nematics. *Phys. Rev. Lett.* **2014**, *113*, 248303.
(48) Giomi, L. Geometry and Topology of Turbulence in Active Nematics. *Phys. Rev. X* **2015**, *5*, 031003.
(49) Zhou, S.; Sokolov, A.; Lavrentovich, O. D.; Aranson, I. S. Living liquid crystals. *Proc. Natl. Acad. Sci. U. S. A.* **2014**, *111*, 1265−1270.
(50) Sokolov, A.; Zhou, S.; Lavrentovich, O. D.; Aranson, I. S. Individual behavior and pairwise interactions between microswimmers in anisotropic liquid. *Phys. Rev. E* **2015**, *91*, 013009.
(51) Kumar, A.; Galstian, T.; Pattanayek, S. K.; Rainville, S. The motility of bacteria in an anisotropic liquid environment. *Mol. Cryst. Liq. Cryst.* **2013**, *574*, 33−39.
(52) Mushenheim, P. C.; Trivedi, R. R.; Tuson, H. H.; Weibel, D. B.; Abbott, N. L. Dynamic self-assembly of motile bacteria in liquid crystals. *Soft Matter* **2014**, *10*, 88−95.
(53) Mushenheim, P. C.; Trivedi, R. R.; Roy, S. S.; Arnold, M. S.; Weibel, D. B.; Abbott, N. L. Effects of confinement, surface-induced orientations and strain on dynamical behaviors of bacteria in thin liquid crystalline films. *Soft Matter* **2015**, *11*, 6821−6831.
(54) Trivedi, R. R.; Maeda, R.; Abbott, N. L.; Spagnolie, S. E.; Weibel, D. B. Bacterial transport of colloids in liquid crystalline environments. *Soft Matter* **2015**, *11*, 8404−8408.
(55) Zhou, S.; Tovkach, O.; Golovaty, D.; Sokolov, A.; Aranson, I. S.; Lavrentovich, O. D. Dynamic states of swimming bacteria in a nematic liquid crystal cell with homeotropic alignment. *New J. Phys.* **2017**, *19*, 055006.
(56) Genkin, M. M.; Sokolov, A.; Lavrentovich, O. D.; Aranson, I. S. Topological defects in a living nematic ensnare swimming bacteria. *Phys. Rev. X* **2017**, *7*, 011029.
(57) Genkin, M. M.; Sokolov, A.; Aranson, I. S. Spontaneous topological charging of tactoids in a living nematic. *New J. Phys.* **2018**, *20*, 043027.
(58) Kawaguchi, K.; Kageyama, R.; Sano, M. Topological defects control collective dynamics in neural progenitor cell cultures. *Nature* **2017**, *545*, 327−331.
(59) Saw, T. B.; Doostmohammadi, A.; Nier, V.; Kocgozlu, L.; Thampi, S.; Toyama, Y.; Marcq, P.; Lim, C. T.; Yeomans, J. M.; Ladoux, B. Topological defects in epithelia govern cell death and extrusion. *Nature* **2017**, *544*, 212−216.
(60) Harvey, C. W.; Alber, M.; Tsimring, L. S.; Aranson, I. S. Continuum modeling of myxobacteria clustering. *New J. Phys.* **2013**, *15*, 035029.

DOI: 10.1021/acs.accounts.8b00300
Acc. Chem. Res. 2018, 51, 3023−3030

(61) Wu, Y.; Kaiser, A. D.; Jiang, Y.; Alber, M. S. Periodic reversal of direction allows Myxobacteria to swarm. *Proc. Natl. Acad. Sci. U. S. A.* **2009**, *106*, 1222−1227.
(62) Kim, Y.-K.; Shiyanovskii, S. V.; Lavrentovich, O. D. Morphogenesis of defects and tactoids during isotropic−nematic phase transition in self-assembled lyotropic chromonic liquid crystals. *J. Phys.: Condens. Matter* **2013**, *25*, 404202.
(63) Zimmermann, N.; Jünnemann-Held, G.; Collings, P. J.; Kitzerow, H.-S. Self-organized assemblies of colloidal particles obtained from an aligned chromonic liquid crystal dispersion. *Soft Matter* **2015**, *11*, 1547−1553.
(64) Pismen, L. Dynamics of defects in an active nematic layer. *Phys. Rev. E* **2013**, *88*, 050502.
(65) Thampi, S. P.; Golestanian, R.; Yeomans, J. M. Instabilities and topological defects in active nematics. *EPL (Europhysics Letters)* **2014**, *105*, 18001.
(66) Zhou, S.; Neupane, K.; Nastishin, Y. A.; Baldwin, A. R.; Shiyanovskii, S. V.; Lavrentovich, O. D.; Sprunt, S. Elasticity, viscosity, and orientational fluctuations of a lyotropic chromonic nematic liquid crystal disodium cromoglycate. *Soft Matter* **2014**, *10*, 6571−6581.
(67) Yasa, O.; Erkoc, P.; Alapan, Y.; Sitti, M. Microalga-Powered Microswimmers toward Active Cargo Delivery. *Adv. Mater.* **2018**, 1804130.
(68) Baraban, L.; Makarov, D.; Streubel, R.; Monch, I.; Grimm, D.; Sanchez, S.; Schmidt, O. G. Catalytic Janus motors on microfluidic chip: deterministic motion for targeted cargo delivery. *ACS Nano* **2012**, *6*, 3383−3389.
(69) Peng, C.; Turiv, T.; Guo, Y.; Wei, Q.-H.; Lavrentovich, O. D. Command of active matter by topological defects and patterns. *Science* **2016**, *354*, 882−885.
(70) Guo, Y.; Jiang, M.; Peng, C.; Sun, K.; Yaroshchuk, O.; Lavrentovich, O.; Wei, Q.-H. High-Resolution and High-Throughput Plasmonic Photopatterning of Complex Molecular Orientations in Liquid Crystals. *Adv. Mater.* **2016**, *28*, 2353−2358.
(71) Hernàndez-Navarro, S.; Tierno, P.; Farrera, J. A.; Ignés-Mullol, J.; Sagués, F. Reconfigurable swarms of nematic colloids controlled by photoactivated surface patterns. *Angew. Chem.* **2014**, *126*, 10872−10876.
(72) Lavrentovich, O. D.; Lazo, I.; Pishnyak, O. P. Nonlinear electrophoresis of dielectric and metal spheres in a nematic liquid crystal. *Nature* **2010**, *467*, 947.
(73) Lavrentovich, O. D. Transport of particles in liquid crystals. *Soft Matter* **2014**, *10*, 1264−1283.
(74) Nazarenko, V.; Boiko, O.; Park, H.-S.; Brodyn, O.; Omelchenko, M.; Tortora, L.; Nastishin, Y. A.; Lavrentovich, O. Surface alignment and anchoring transitions in nematic lyotropic chromonic liquid crystal. *Phys. Rev. Lett.* **2010**, *105*, 017801.
(75) Ebbens, S. J.; Howse, J. R. In pursuit of propulsion at the nanoscale. *Soft Matter* **2010**, *6*, 726−738.
(76) Bukusoglu, E.; Bedolla Pantoja, M.; Mushenheim, P. C.; Wang, X.; Abbott, N. L. Design of responsive and active (soft) materials using liquid crystals. *Annu. Rev. Chem. Biomol. Eng.* **2016**, *7*, 163−196.
(77) Mangal, R.; Nayani, K.; Kim, Y.-K.; Bukusoglu, E.; Córdova-Figueroa, U. M.; Abbott, N. L. Active Janus Particles at Interfaces of Liquid Crystals. *Langmuir* **2017**, *33*, 10917−10926.
(78) Wang, W.; Castro, L. A.; Hoyos, M.; Mallouk, T. E. Autonomous motion of metallic microrods propelled by ultrasound. *ACS Nano* **2012**, *6*, 6122−6132.
(79) Wang, W.; Li, S.; Mair, L.; Ahmed, S.; Huang, T. J.; Mallouk, T. E. Acoustic propulsion of nanorod motors inside living cells. *Angew. Chem., Int. Ed.* **2014**, *53*, 3201−3204.
(80) Ghosh, A.; Fischer, P. Controlled propulsion of artificial magnetic nanostructured propellers. *Nano Lett.* **2009**, *9*, 2243−2245.
(81) Kléman, M. Energetics of the focal conics of smectic phases. *J. Phys. (Paris)* **1977**, *38*, 1511−1518.
(82) Guo, W.; Herminghaus, S.; Bahr, C. Controlling smectic focal conic domains by substrate patterning. *Langmuir* **2008**, *24*, 8174−8180.
(83) Guillamat, P.; Ignés-Mullol, J.; Sagués, F. Taming active turbulence with patterned soft interfaces. *Nat. Commun.* **2017**, *8*, 564.
(84) Guillamat, P.; Ignés-Mullol, J.; Sagués, F. Control of active liquid crystals with a magnetic field. *Proc. Natl. Acad. Sci. U. S. A.* **2016**, *113*, 5498−5502.
(85) Drescher, K.; Dunkel, J.; Cisneros, L. H.; Ganguly, S.; Goldstein, R. E. Fluid dynamics and noise in bacterial cell−cell and cell−surface scattering. *Proc. Natl. Acad. Sci. U. S. A.* **2011**, *108*, 10940−10945.
(86) Wang, W.; Duan, W.; Ahmed, S.; Sen, A.; Mallouk, T. E. From one to many: Dynamic assembly and collective behavior of self-propelled colloidal motors. *Acc. Chem. Res.* **2015**, *48*, 1938−1946.
(87) Viney, C.; Huber, A. E.; Verdugo, P. Liquid-crystalline order in mucus. *Macromolecules* **1993**, *26*, 852−855.
(88) Smalyukh, I. I.; Zribi, O. V.; Butler, J. C.; Lavrentovich, O. D.; Wong, G. C. Structure and dynamics of liquid crystalline pattern formation in drying droplets of DNA. *Phys. Rev. Lett.* **2006**, *96*, 177801.
(89) Dogic, Z.; Fraden, S. Ordered phases of filamentous viruses. *Curr. Opin. Colloid Interface Sci.* **2006**, *11*, 47−55.
(90) Figueroa-Morales, N.; Dominguez-Rubio, L.; Ott, T. L.; Aranson, I. S. Mechanical shear controls bacteria penetration in mucus. *Proc. Natl. Acad. Sci. U. S. A.*, submitted, **2018**.

DOI: 10.1021/acs.accounts.8b00300
Acc. Chem. Res. 2018, 51, 3023−3030